NAZARBAYEV UNIVERSITY

FUNCTIONAL ASSESSMENT OF A JP342 FLUORESCENT PROBE FOR CATHEPSIN G DETECTION IN TUMOR CELLS

Aiya Makhanova

(B.Sc., Nazarbayev University)

A THESIS SUBMITTED

FOR THE DEGREE OF MASTER OF LIFE SCIENCES

DEPARTMENT OF BIOLOGY SCHOOL OF SCIENCES AND HUMANITIES

NAZARBAYEV UNIVERSITY

2025

Student: Aiya Makhanova  17 April 2025

DECLARATION

I hereby declare that the thesis is my original work and it has been written by me in its entirety. I have duly acknowledged all the sources of information which have been used in the thesis. This thesis has also not been submitted for any degree in any university previously.

Aiya Makhanova

17 April, 2025

ACKNOWLEDGEMENTS

I would like to express my sincere gratitude to my principal investigator and project supervisor, Professor Timo Burster, for his guidance and continuous support throughout this work. His advice and encouragement carried me through each stage of the project. I am truly grateful for the opportunity to be a part of the Laboratory of Immunology.

I would also like to thank Professor Steven Verhelst, a collaborator of our laboratory, for providing the novel fluorescent probe JP342 that served as the cornerstone of this project.

Lastly, I wish to thank my colleagues in the laboratory for their helpful discussions and kind assistance during the course of my research.

TABLE OF CONTENTS

ABSTRACT

Cathepsin G (CatG) is a serine protease secreted by activated neutrophils that performs essential functions related to immune defense, inflammation, and cancer. Accurately detecting its enzymatic activity is crucial for understanding the role of CatG in health and disease. This project assesses an innovative boron-dipyrromethene (BODIPY) labeled activity-based probe JP342 for the detection of CatG, while comparing its efficacy with the established MARS116-FAM probe across different experimental conditions. Of these, SDS-PAGE, flow cytometry, and confocal microscopy were applied to both JP342 and MARS116-FAM. JP342 and MARS116-FAM exhibited a concentration-dependent affinity for labeling purified CatG, with MARS116-FAM showing greater sensitivity at all tested concentrations in gel-based assays and confocal microscopy. In contrast, the flow cytometry analysis determined that JP342 exhibited a markedly elevated median fluorescence intensity (MFI), irrespective of the presence of a CatG-specific inhibitor, which suggests a higher affinity of JP342 towards CatG in flow cytometry. Overall, the findings indicate that JP342 serves as a compelling activity-based probe for detecting CatG activity in flow cytometry applications, while MARS116-FAM continues to demonstrate optimal performance in gel-based assays and cell imaging. These results emphasize the importance of matching the activity-based probe to the type of experiment.

LIST OF FIGURES

ABBREVIATIONS

CatG	cathepsin G
NE	neutrophil elastase
CatG inh I	cathepsin G inhibitor
PMNs	polymorphonuclear neutrophils
CTLs	cytotoxic T lymphocytes
COPD	chronic obstructive pulmonary disease
PLTP	phospholipid transfer protein
RA	rheumatoid arthritis
TFPI	tissue factor pathway inhibitor
RAGE	receptor for advanced glycation end products
Tsp-1	thrombospondin-1
ABPP	activity-based protein profiling
ABPs	activity-based probes
BODIPY-FL	boron-dipyrromethene fluorescein-like
qABP	quenched fluorescent activity-based probe

1 INTRODUCTION

1.1 Cathepsin G (CatG): Structure, Function, and Roles in Immunity

1.1.1 Structural features and catalytic mechanism of CatG

Cathepsin G (CatG) is a 30 kDa serine protease that belongs to the family of S1 peptidases. It shares homology with cytotoxic T lymphocyte (CTL) associated granzymes and tryptase and chymase enzymes expressed by mast cells. CatG is predominantly produced by polymorphonuclear neutrophils (PMNs), where it is stored in azurophilic granules (also known as primary granules) alongside other proteolytic enzymes such as neutrophil elastase (NE) or proteinase 3 (PR3) (Pham, 2006). These proteases are essential for the innate immune system's ability to mount rapid responses against invading pathogens.

CatG exhibits a preference for hydrolyzing peptide bonds adjacent to specific amarcinmino acids at the P1 position, including basic residues such as lysine (K) and arginine (R); aromatic residues like phenylalanine (F), tyrosine (Y), and tryptophan (W), which corresponds to mix of trypsin and chymotrypsin proteolytic activities. In addition, CatG can hydrolyze the peptide bond after leucine (L) (Burster et al., 2021). Regarding the enzymatic activity of CatG, it is structurally characterized by a classical serine protease catalytic triad composed of serine (S195), histidine (H57), and aspartate (D102) amino acid residues (Korkmaz et al., 2010). The serine hydroxyl group acts as a potent nucleophile following proton abstraction by histidine, enabling it to attack the substrate's amide bond. This reaction forms a temporary tetrahedral intermediate which is later broken by hydrolysis, resulting in the release of the cleaved peptide and the restoration of the protease to its active form (Figure 1).

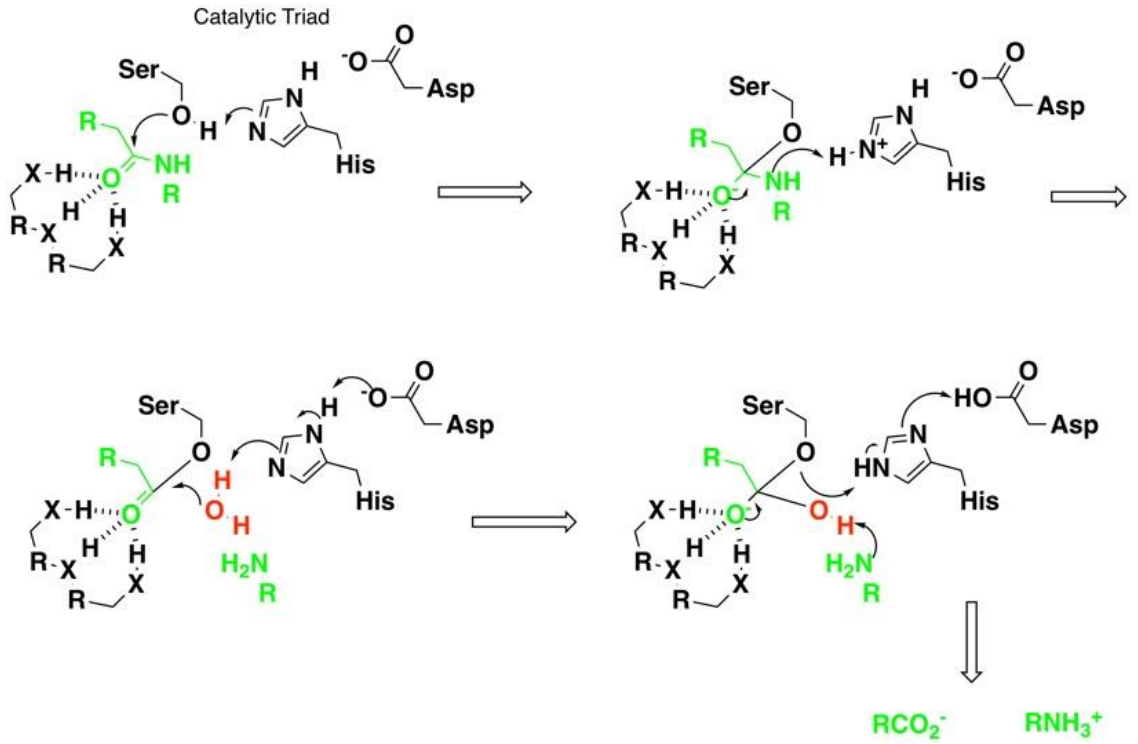

Figure 1. Catalytic mechanism of serine proteases (Adapted from Swain, Cambridge MedChem Consulting, 2012)

1.1.2 Role of CatG in immune defense

This catalytic activity of CatG plays a significant role in the degradation of proteins, particularly in relation to immune defense. Upon neutrophil activation, CatG and other serine proteases can be released extracellularly during infection, inflammation, or tissue damage. CatG targets and breaks down microbial proteins, thus participating in pathogen clearance (Pham, 2006). Furthermore, CatG is involved in immune regulation through its ability to process and activate cytokines, chemokines, and growth factors, which mobilize and activate immune cells at sites of infection. It has been shown to convert pro-IL-1β into its active form and activate other immune mediators like TNF-α, hence amplifying the inflammatory response (Conus & Simon, 2010). Moreover, CatG activates metalloproteinases and cleaves extracellular matrix proteins, facilitating neutrophil migration. Taken together, CatG serves as a multifunctional enzyme that not only contributes to direct pathogen killing but also plays a broader role in immune modulation and tissue remodeling.

1.2 CatG in Pathology: Inflammation and Tumorigenesis

1.2.1 CatG's involvement in inflammatory diseases

While CatG plays critical protective roles in immune defense, its dysregulation is increasingly recognized as a contributor to pathological inflammation and tissue damage. Excessive release of CatG from activated neutrophils, along with impaired regulation by natural inhibitors (serpins), has been implicated in a wide range of chronic inflammatory and autoimmune diseases (Zamolodchikova et al., 2020). For instance, in chronic obstructive pulmonary disease (COPD), CatG has been shown to degrade phospholipid transfer protein (PLTP), a protective anti-inflammatory factor, thereby amplifying pulmonary inflammation and enhancing neutrophil-mediated tissue damage (Brehm et al., 2014).

In rheumatoid arthritis (RA), a prototypical autoimmune disorder characterized by chronic joint inflammation and progressive cartilage destruction, CatG has been found at elevated levels in synovial fluid and inflamed joint tissues. Miyata et al. (2006) demonstrated that CatG can serve as a chemoattractant for monocytes, increasing immune cell infiltration and inflammation. Moreover, CatG may contribute to cartilage degradation both directly through the proteolysis of extracellular matrix components such as fibronectin and indirectly via the activation of pro-inflammatory cytokines like TNF-α and IL-1β.

CatG also plays a role in cardiovascular diseases, particularly atherosclerosis. In this context, CatG secreted by neutrophils that adhere to endothelial cells can cleave components of the extracellular matrix, destabilize plaques, and promote thrombus formation. Ortega-Gomez et al. (2016) demonstrated that in mice lacking CatG, the development of atherosclerotic plaques was significantly reduced. This reduction was linked to decreased leukocyte adhesion and migration, largely due to diminished integrin activation on endothelial surfaces. Additionally, CatG can function synergistically with neutrophil elastase (NE) to degrade tissue factor pathway inhibitor (TFPI), thereby enhancing thrombogenicity and accelerating plaque rupture (Kurup & Patel, 2017).

1.2.2 Dual role of CatG in cancer

In cancer, the role of CatG is paradoxical — it can exert both tumor-promoting and tumor-suppressive effects depending on the context. For instance, CatG has been shown to enhance tumor immune surveillance through the recognition of tumor-expressed receptors. A study by Sionov et al. (2019) demonstrated that CatG can bind to the receptor for advanced glycation

end products (RAGE) on tumor cells, promoting neutrophil-mediated cytotoxicity and inhibiting tumor growth. This highlights a potentially beneficial role for CatG in anti-tumor immunity. Conversely, other evidence suggests that CatG can contribute to tumor progression. Rayes et al. (2015) reported that CatG, in combination with NE, degrades thrombospondin-1 (TSP-1), an anti-angiogenic factor that also functions as a tumor suppressor. The degradation of TSP-1 promotes angiogenesis and facilitates tumor cell extravasation and metastatic colonization, especially in lung metastasis models. Such findings imply that the net effect of CatG in cancer depends on the tumor microenvironment, its interaction with other proteases, and the balance between immune surveillance and immune evasion.

The duality of CatG's role in cancer and inflammation needs further investigation. Therefore, tracking the proteolytic active CatG is essential for understanding its role in pathology.

1.3 Activity-Based Probes as Tools for CatG Detection

Traditional biochemical approaches such as ELISA and Western blotting are widely used to detect proteases like CatG by measuring their protein levels. However, these methods detect only total protein (inactive zymogen, active enzyme, or proteolytic inhibited enzyme) and cannot distinguish between catalytically active and inactive forms. This limitation becomes critical in biological systems where only the active form of a protease exerts functional effects. To overcome this, **activity-based probes (ABPs)** have emerged as innovative tools to assess real-time functional activity in complex biological samples and systems.

Activity-based protein profiling (ABPP) utilizes ABPs designed to bind covalently and irreversibly to the catalytic site of active enzymes. These probes typically consist of three major components:

- **A reactive group** (warhead), which targets the serine residue on the catalytic site of the protease;
- **A recognition sequence or linker**, which provides selectivity by mimicking natural substrates;
- **A reporter tag**, such as a fluorophore, that enables detection (Figure 2).

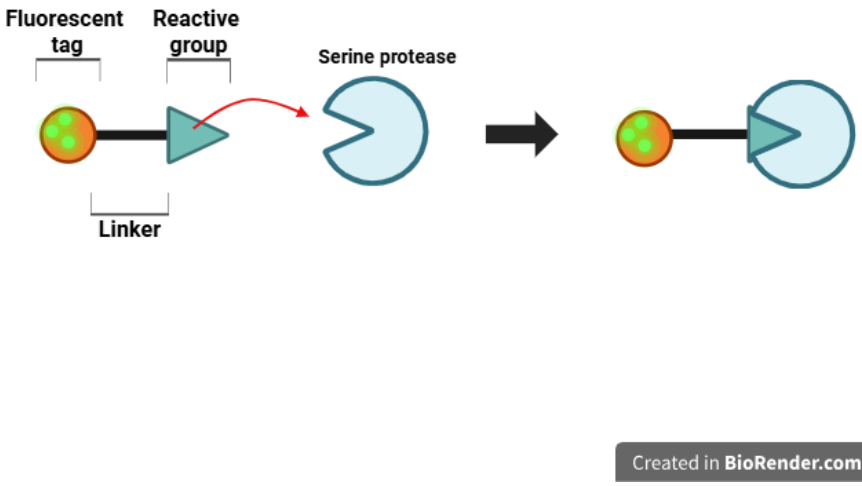

Figure 2. The schematic representation of ABPs and their interaction with serine proteases (The scheme was created using BioRender.com)

In the context of CatG, this approach enables precise spatial and temporal visualization of proteolytic activity. Furthermore, ABPs can be applied in live-cell systems, allowing to monitoring of dynamic processes such as inflammation or tumor progression.

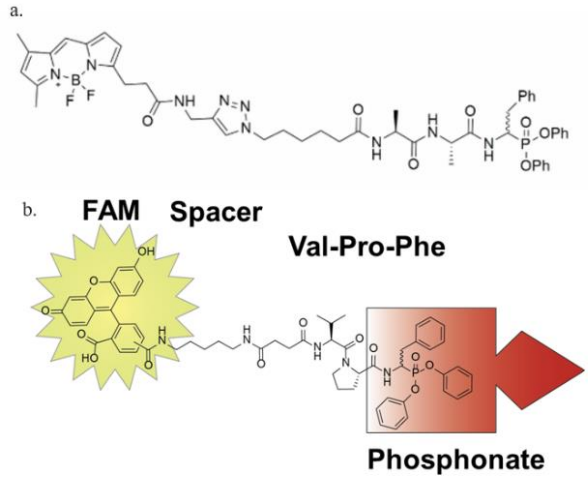

Figure 3. The chemical structure of **a)** JP342 and **b)** MARS116-FAM activity-based probes

One such probe, **MARS116-FAM** (Figure 3b), has been employed to detect CatG in primary immune cells, including CD4+ and CD8+ T cells (Schroeder et al., 2019), as well as epithelial cancer cell lines such as A549 (Assylbekova et al., 2024). MARS116-FAM carries a fluorescein-based tag (FAM) that permits visualization under standard fluorescent microscopes and flow cytometry assays.

To explore alternative strategies, this study introduces **JP342**, a novel probe incorporating a boron-dipyrromethene fluorescein-like (BODIPY-FL) reporter tag (Figure 3a). BODIPY-FL is known for its high quantum yield, narrow emission spectrum, and enhanced photostability compared to FAM. These features may offer advantages in certain applications, such as enhanced signal-to-noise ratios or increased stability during imaging. In addition, JP342 includes a triazole-containing linker, which enhances chemical stability and may reduce enzymatic degradation in the cellular environment (Matin et al., 2022).

This probe has not yet been widely tested in cancer-related systems, especially in comparison with established probes like MARS116-FAM. By incorporating enzyme inhibitors as controls and optimizing probe concentrations, this study seeks to validate JP342 as a reliable tool for live-cell imaging and quantitative analysis of CatG activity.

2 MATERIALS AND METHODS

2.1 Cell culturing

One cell line was utilized for the project, referred to as A549 (CCL-185, American Type Culture Collection, ATCC, Manassas, VA, USA), which is an adherent human adenocarcinoma alveolar basal epithelial tumor cell line. The cells were cultured in RPMI-1640 complete medium (R8755-1L, Lot No. SLBF1516V, Sigma-Aldrich, St. Louis, MO, USA), supplemented with 10% heat-inactivated fetal bovine serum (FBS, Lot No. 2631713RP, Gibco, Grand Island, NY, USA) and 1% of a mixture of penicillin G and streptomycin (pen-strep, Lot No. 210496, Gibco, Grand Island, NY, USA). For propagation purposes, the cells were cultured in 60 mm dishes. The adherent cell line was aspirated, and the cells were washed with PBS (pH 7.4, Lot No. RNBL5991, Sigma-Aldrich, St. Louis, MO, USA). For detachment, trypsin 1X EDTA (Lot No. 2537762, Gibco, Grand Island, NY, USA) was applied in an appropriate volume corresponding to the size of the dish, and the cells were incubated for 5 minutes in the incubator (Thermo Fisher Scientific, Waltham, MA, USA) which is supplied with CO_2 gas at a temperature of 37°C. Complete RPMI-1640 was used to neutralize trypsin, and the cells were collected into 15 ml tubes. A549 cells were centrifuged at 250 to 300 x g for 5 minutes (Model C 2201, Liston LLC, Russia). The passage of A549 was performed every 2 to 3 days to 0.7×10^6 cells/mL.

For experiments with flow cytometry analysis, A549 cells were seeded using 100 mm dishes with a density of 0.15×10^7 to 0.2×10^7 cells per dish.

For confocal imaging, cells were plated on 8-well chamber slides (Sarstedt AG & Co. KG, Nümbrecht, Germany) with a seeding density of 0.5×10^5 cells per well.

To prepare cell lysates, A549 were seeded into 60 mm dishes at a cell density of 0.8×10^6 cells to 0.1×10^7 cells to achieve the necessary number of cells for lysis and protein content.

2.2 Sample Processing and Workflow for Gel-Based Detection

Assessment of CatG concentration-dependent probe labeling efficiency

To determine the optimal concentration of CatG (PN: 16-14-030107, Lot No. CG 2023-01, Athens Research and Technology, Athens, GA, USA) required for activity-based probe detection, a titration of the protease was performed using four concentrations: 40 µg/mL, 20 µg/mL, 10 µg/mL, and 5 µg/mL. In total, eight 1.5 mL Eppendorf tubes were prepared for the experiment. After adding the titrated CatG solutions, JP342 and MARS116-FAM were added to the samples at a final concentration of 10 µM. The JP342 was kindly provided by Professor Dr. Steven Verhelst, while MARS116-FAM was given by Professor Dr. Marcin Sienczyk and

Professor Dr. Renata Grzywa. The mixtures were incubated for 45 minutes in the dark to protect the fluorescent probe from light exposure. The activity-based probe MARS116-FAM was used as a reference probe.

Titration of JP432 probe for CatG detection

For the titration of the probe, a mastermix containing CatG [40 µg/mL], diluted from stock (1 µg/µL), was prepared in PBS and distributed equally among six 1.5 mL Eppendorf tubes. JP342 was titrated in a series of five concentrations: 10 µM, 5 µM, 2.5 µM, 1.25 µM, and 0.625 µM. For comparison, MARS116-FAM [10 µM] was included based on previous research data. JP342 was added and sequentially diluted to achieve the required concentrations. All tubes were incubated in the dark for 45 minutes.

Evaluation of probe sensitivity to CatG inhibition

To assess the functional specificity of the novel probe, CatG inhibitor I (CatG inh I, Calbiochem Research Biochemicals, Schwalbach, Germany) was utilized. A mastermix with CatG inh I [50 µM] and CatG [40 µg/mL] was prepared in PBS and incubated for 15 minutes at room temperature (RT). After pre-incubation, JP342 [10 µM] and MARS116-FAM [10 µM] probes were added and diluted four times: 10 µM, 5 µM, 2.5 µM, and 1.25 µM, and incubated for an additional 45 minutes in the dark. The samples with CatG [40 µg/mL] and probe [10 µM] only served as a positive control.

SDS-PAGE and detection protocol

Following incubation, each reaction mixture from three separate experiments was supplemented with 6x protein loading buffer (30% glycerol, stacking buffer, 6 mM EDTA, 10% SDS, 60 mM DTT, Bromphenol Blue), gently mixed, and heated at 95°C for 5 minutes to reduce and denature the proteins.

All samples for experiments were then processed according to the SDS-PAGE protocol (NeoBiotechnologies, 2024). Detection of the fluorescent signal was performed using the Chemidoc MP imaging system (Bio-Rad Laboratories, Hercules, CA, USA) with the Emerald 488 filter. Coomassie Blue staining (Cat. No. 1610786, Bio-Rad Laboratories, Hercules, CA, USA) was used to visualize protein bands and confirm the presence of CatG at approximately 30 kDa. Destaining with a solution of 40 % ethanol and 10% acetic acid was carried out for 12 hours, and stained gels were imaged using the Chemidoc.

2.3 FACS analysis of CatG on the cell Surface of A549 Cells using activity-based probes and inhibitor:

Two mastermix were prepared for the experiment: one containing CatG at a final concentration of [10 μg/mL] and PBS (pH 7.4); the other containing CatG [10 μg/mL], PBS, and CatG inh I [100 uM]. The mixture with the inhibitor was incubated for 15 minutes, and distributed to 1.5 mL Eppendorf tubes. One tube was used as a control without any probe. JP342 and MARS116-FAM probes were added to designated tubes, titrated, and incubated for 45 minutes in the dark at RT. The appropriate amount of A549 cells (0.3×10^7 cells) was measured and added to 1.5 mL tubes and incubated for 1 hour. For centrifugation, 5 minutes at a speed of 250 x g was used. Cells were washed twice with 200 μL of FACS buffer (PBS pH 7.4 and 1% FBS) and centrifuged twice at the same speed and time. To distinguish live and apoptotic cells, A549 cells were resuspended in 200 μL of FACS buffer and stained with propidium iodide (PI) at a concentration of 0.5 μg/mL. The cells were collected and analyzed using an Attune Nxt Flow Cytometer (Thermo Fisher Scientific, Waltham, MA, USA). The obtained data were processed with FlowJo™ v10.8.1 Software (BD Life Sciences, Ashland, OR, USA). Detection of PI was determined using the Yl2-A channel, while probe functionality was tested utilizing the BL1-A channel. Control samples with CatG inh I were used to validate the specificity of the activity-based probes.

The gating strategy was based on the forward versus side scatter (FSC/SSC) profile to exclude debris. Single cells were isolated using forward scatter height (FSC-H) compared with forward scatter area (FSC-A). Median fluorescence intensity (MFI) from the BL1-A channel was used for statistical analysis.

2.4 Confocal imaging of A549 cells treated with CatG via application of activity-based probes and inhibitor controls

Prior to the experiment, A549 cells were seeded on an 8-well cell culture chamber slides with RPMI-1640 complete medium (10% FBS, 1% pen-strep) for 24 h. Next, a mastermix containing CatG [10 μg/mL] was prepared in RPMI-1640 serum-free medium (0% FBS) and distributed to 1.5 ml Eppendorf tubes. Activity-based probes such as JP342 and MARS116-FAM were added to tubes with varying concentrations of 5 and 2.5 μM. Two controls were used for each probe: one was prepared with only probe [5 μM]; the second one was done using CatG [10 μg/mL], the probe and CatG inh I [50 μM]; both were mixed with RPMI-1640 serum-free medium. The protease and ABP were incubated for 45 min at RT and protected from light.

Afterward, the protease–ABP complex was added to the A549 cells. The cells were washed several times with PBS (pH 7.4) and fixed in ice-cold 99% methanol for 5 minutes. To remove the effect of methanol, A549 cells were washed with PBS three times. Then, Hoechst dye (Cayman Chemical, Ann Arbor, MI, USA) with a concentration of [10 μg/mL] was applied to cells on slides for 10 min before confocal microscopy analysis. For the visualization of protease-ABP complex within cells, ZEISS LSM 780 (Carl Zeiss AG) was utilized. Hoechst was detected using the DAPI channel (405 nm), and activity-based probes were detected with the FITC channel (488 nm). Both channels for image generation were captured sequentially. All acquired images were analyzed by ImageJ software (version 1.54f, NIH, USA).

2.5 The apoptosis profiler array for A549 cells treated with CatG

A549 cells cultured on 60 mm dishes with confluency of 70-80% were treated with CatG [10 μg/mL] under serum-free conditions for 16 hours. A549 without CatG served as a control. Afterward, cells were trypsinized, and a dry pellet was collected into 15 ml tubes. Cells were lysed according to the protocol from R&D Systems for Human Apoptosis Antibody Array Kit (Cat. No. ARY009, Lot No. 1718009, R&D Systems, Minneapolis, MN, USA). For apoptosis, Lysis buffer 17 was used with an inhibitor mix containing Aprotinin [10 μM] (Cat. No. 4139, Tocris Bioscience, UK), Leupeptin hemisulfate [10 μM] (Cat. No. 1167, Tocris Bioscience, UK), and Pepstatin A [10 μM] (Cat. No. 1190, Tocris Bioscience, UK). The cell lysates were kept on ice for 30 minutes, centrifuged at 14000xg for 5 minutes, and the supernatant was collected for Bradford assay.

Bradford assay was performed on a 96-well plate to estimate the protein content in supernatants using Quick Start™ Bradford 1x Dye (Cat. No. 5000205, Bio-Rad Laboratories, Hercules, CA, USA). The data was collected with the Varioskan Flash apparatus (Thermo Fisher Scientific, Waltham, MA, USA), and the data was analyzed in Microsoft Excel.

The Human Apoptosis Antibody Array Kit was used to semi-quantitatively assess the expression of apoptosis-related proteins. Before use, array membranes were placed into wells of a 4-well multi-dish containing 2 mL of Array Buffer 1 for blocking. Array membranes were incubated for 1 hour at RT on a shaker. Samples were prepared by mixing cell lysates (150 μg) with Array Buffer 1 to a total volume of 1.5 mL. After blocking, the buffer was aspirated, and prepared samples were added to the membranes. Array membranes were incubated overnight at 4 °C on a shaker. The next day, array membranes were washed three times with 1x Wash Buffer for 10 minutes. Detection Antibody Cocktail was diluted in Array Buffer 2/3 and added to each array membrane (1.5 mL/well) and followed by 1-hour incubation at RT. Then, arrays

were washed and incubated with diluted Streptavidin-HRP solution (1:2000) for 30 minutes and washed 3 additional times. Next, 1 mL of Chemi Reagent Mix was applied to each array membrane. Chemiluminescence was visualized through the Chemidoc MP detector (Bio-Rad Laboratories, Hercules, CA, USA).

2.6 Statistical data analysis

Generated data was analyzed through GraphPad Prism 10.2.3 (San Diego, CA, USA) using appropriate statistical tests for collected data from different methods. For flow cytometry data, fluorescence intensity values (MFI) were analyzed using two-way ANOVA when assumptions of normality and homogeneity of variance were met (through Shapiro-Wilk and Levene's tests). Outliers were identified and removed using the ROUT method where appropriate. When assumptions were violated, the Aligned Rank Transform (ART) ANOVA was conducted in R. For post hoc pairwise comparisons analysis, Sidak's method was conducted.

Gel electrophoresis band intensities were extracted using ImageJ by measuring the area under curve (AUC) of probe-labeled bands. Data were analyzed via two-way ANOVA.

Confocal microscopy images were assessed qualitatively in ImageJ. Due to the limited sample size and the visual nature of imaging, no statistical tests were applied; however, fluorescence patterns and probe localization were interpreted descriptively.

3 AIMS OF THE THESIS PROJECT

The **hypothesis** for this project is that the novel BODIPY-based JP342 activity-based probe will effectively bind and detect active CatG and perform as well as, or better than, the established MARS116-FAM probe in different experimental settings. This study will help determine if JP342 can serve as a reliable tool for detecting CatG activity, particularly in tumor cells.

To investigate the efficacy of JP342 as a detection tool for CatG activity, the study seeks to achieve several aims:

Aim 1. Optimize and validate the novel JP342 probe for CatG detection using gel-based analysis

Objectives:

- To assess concentration-dependent JP342 probe labeling efficiency across different CatG concentrations.
- To determine the optimal probe concentration for CatG detection.
- To evaluate the probe's sensitivity to CatG inhibition.

Aim 2. Evaluate the sensitivity and specificity of the JP342 probe in detecting CatG activity on the cell surface using flow cytometry

Objectives**:**

- To compare JP342 and MARS116-FAM probes' binding to A549 cells treated with exogenous CatG.
- To assess probe specificity using CatG inhibitor treatment.
- To analyze probe signal strength via quantification of median fluorescence intensity (MFI).

Aim 3. Visualize and validate CatG activity in A549 cells using confocal microscopy

Objectives**:**

- To compare cellular localization of JP342 and MARS116-FAM probes upon CatG treatment.

- To evaluate the effect of probe concentration and CatG inhibition on intracellular fluorescence signal.

4 RESULTS

4.1 Exogenous CatG treatment does not induce apoptosis in A549 cells.

To ensure that protease treatment does not affect A549 cell viability in subsequent flow cytometry and confocal microscopy experiments, an apoptosis array was performed under serum-free conditions for 16 hours. According to the data, no signal corresponding to apoptotic markers such as pro-caspase 3 or active caspase 3 was detected (Figure 4). The absence of these markers indicates that CatG treatment did not induce apoptotic signaling in A549 cells, which means that the cells remained viable throughout the experiment.

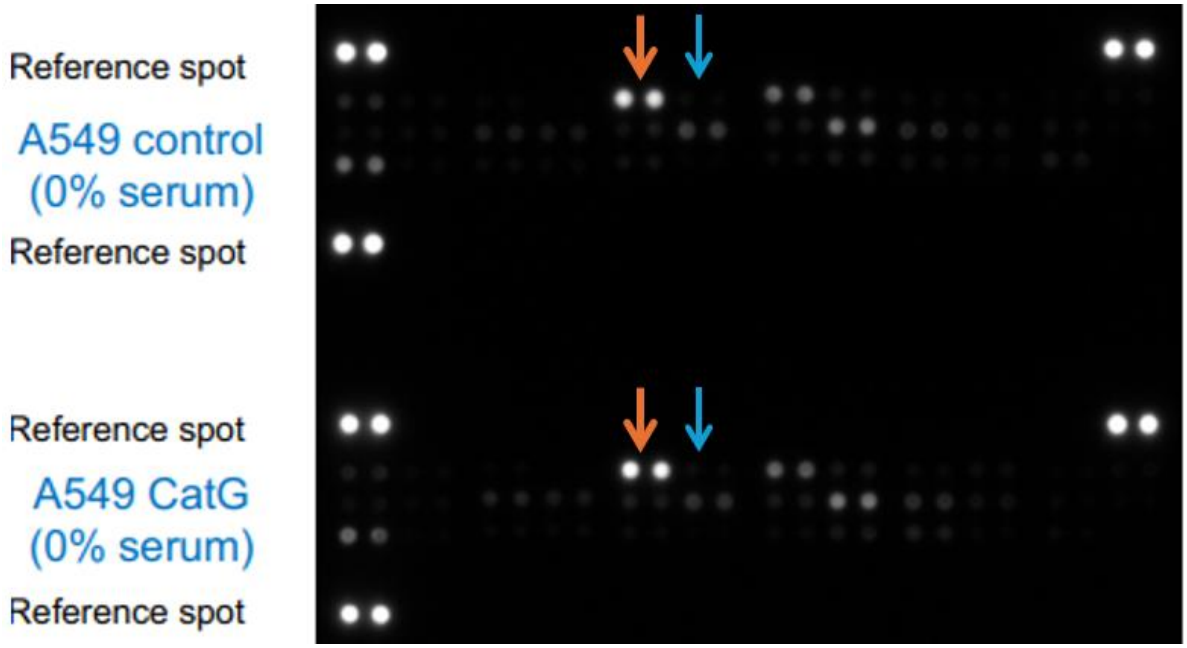

Figure 4. Apoptosis profiler array of A549 cells incubated with CatG [10 µg/mL] in serum-free medium for 16 hours (Orange color represents pro-caspase 3 and blue color shows cleaved caspase 3).

4.2 MARS116-FAM is a more sensitive activity-based probe in contrast to JP342 for detecting catalytically active CatG.

To assess probe performance to bind to the catalytic center of CatG, the protease was titrated (four concentrations, 5–40 µg/mL) while maintaining a constant concentration for the novel activity-based probe JP342 and MARS116-FAM as indicated in Figure 5. According to the data, both probes demonstrated increasing fluorescence intensity with higher CatG

concentrations. Statistical analysis revealed that MARS116-FAM consistently generated a stronger signal than JP342, with a significant difference observed at 40 µg/mL of CatG. The loading control, coomassie staining, confirmed a progressive decrease in total protein, which corresponds to the CatG dilution, and it validates the observed differences in fluorescence.

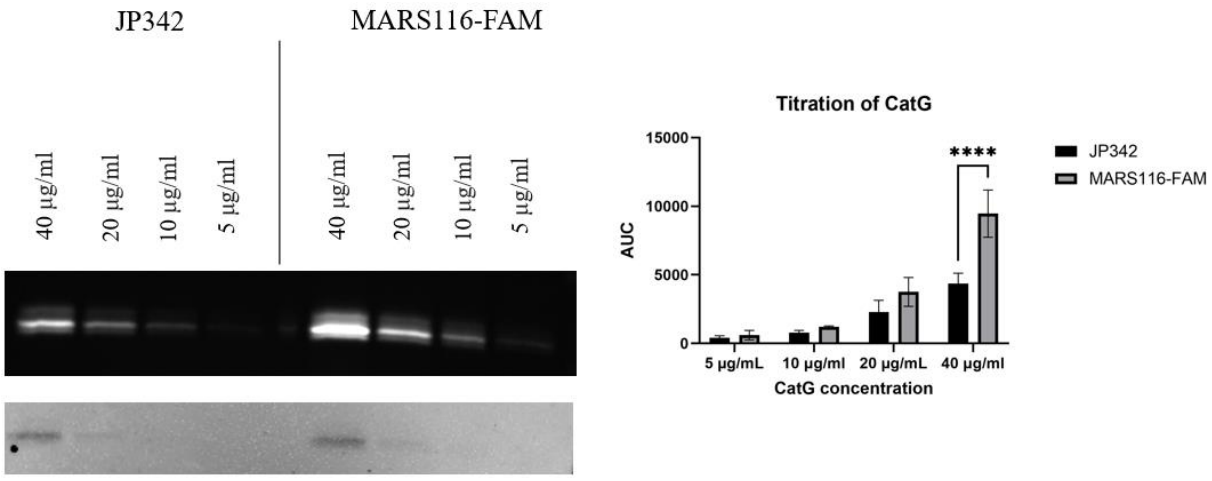

Figure 5. SDS-PAGE analysis showing labeling of increasing concentrations of CatG [5–40 µg/mL] using JP342 and MARS116-FAM probes [10 µM] at constant concentration. Fluorescent signals (upper panel) were visualized in the Emerald 488 channel. Coomassie staining (lower panel) confirms total protein presence. On the right panel, quantified band intensities are shown as the area under the curve (AUC) from three replicates. Data was analyzed using 2-way ANOVA and Sidak post hoc test (****$p \leq 0.0001$). Values represent mean ± SD, n = 3.

To compare the fluorescent labeling efficiency of JP342 and MARS116-FAM, each probe was titrated across a range of concentrations [10–0.625 µM] while incubated with CatG at a constant concentration [40 µg/mL]. As shown in Figure 6, fluorescence imaging of SDS-PAGE gels revealed a concentration-dependent decrease in band intensity for both probes. Quantitative analysis demonstrated that MARS116-FAM consistently showed higher fluorescence signals compared to JP342 at equal concentrations, with significant differences at 5 µM and 10 µM. Thus, MARS116-FAM binds with higher affinity to the catalytic center of CatG in contrast to JP342.

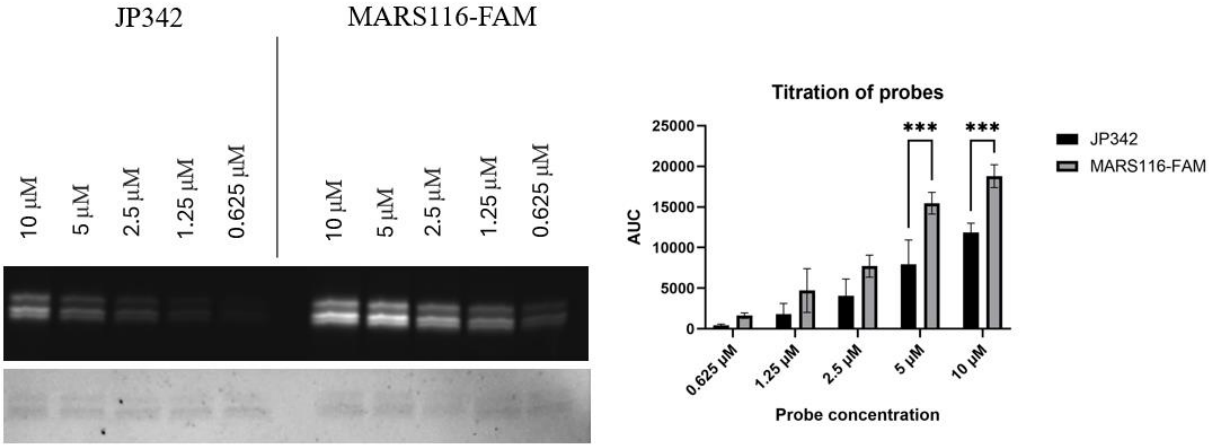

Figure 6. Detection of CatG activity using titrated JP342 and MARS116-FAM probes via SDS-PAGE. Fluorescence gel (upper panel) shows labeling of CatG [40 µg/mL] with decreasing probe concentrations [10–0.625 µM]. Coomassie-stained gel (lower panel) confirms uniform protein loading. Quantified band intensities (right panel) are presented as the area under the curve (AUC) from three independent experiments. Data was analyzed using 2-way ANOVA and Sidak post hoc test with significance shown at each probe concentration (*** $p \leq 0.001$). Values represent mean ± SD, n = 3.

An additional control was performed to demonstrate specific binding of the probes to CatG. In samples treated with the CatG inh I, the fluorescence signal was substantially diminished for both probes, supporting their specificity for active CatG (Figure 7).

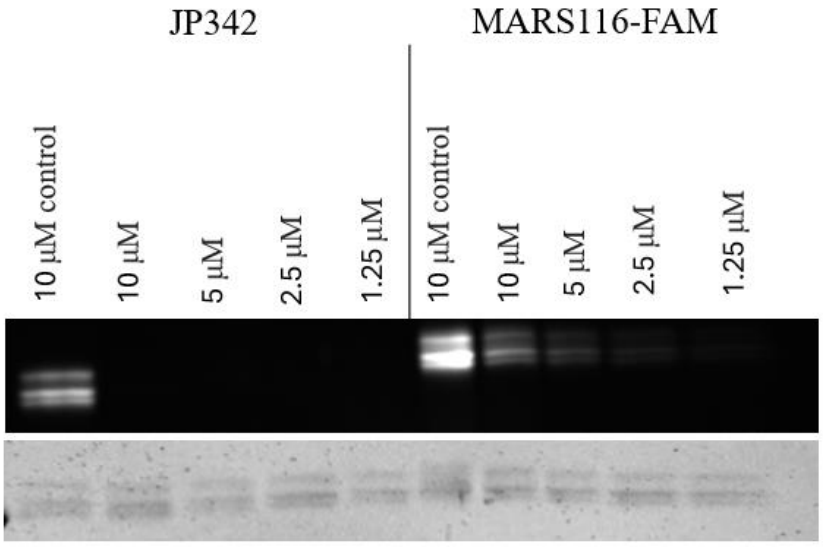

Figure 7. SDS-PAGE analysis showing fluorescence signal of JP342 and MARS116-FAM probes titrated at decreasing concentrations [10–1.25 µM] in the presence of CatG [40 µg/mL] with CatG inh I [50 µM]. The first lane for each probe represents a control condition containing CatG and the probe

only. Upper panel: fluorescent scan using the Emerald 488 channel. Lower panel: Coomassie staining to confirm equal CatG loading across lanes.

4.3 JP342 labels CatG with higher affinity in contrast to MARS116-FAM, as analyzed by flow cytometry.

In the absence of the CatG inh I (Figure 8), both JP342 and MARS116-FAM showed a dose-dependent increase in median fluorescence intensity (MFI), which indicates an effective labeling of CatG present on the cell surface. However, at concentrations starting from 1 µM and higher, JP342 consistently generated significantly higher MFI values compared to MARS116-FAM, with the strongest signal observed at 10 µM. Thus, JP342 demonstrates a higher affinity to CatG in contrast to MARS-116-FAM by using flow cytometry.

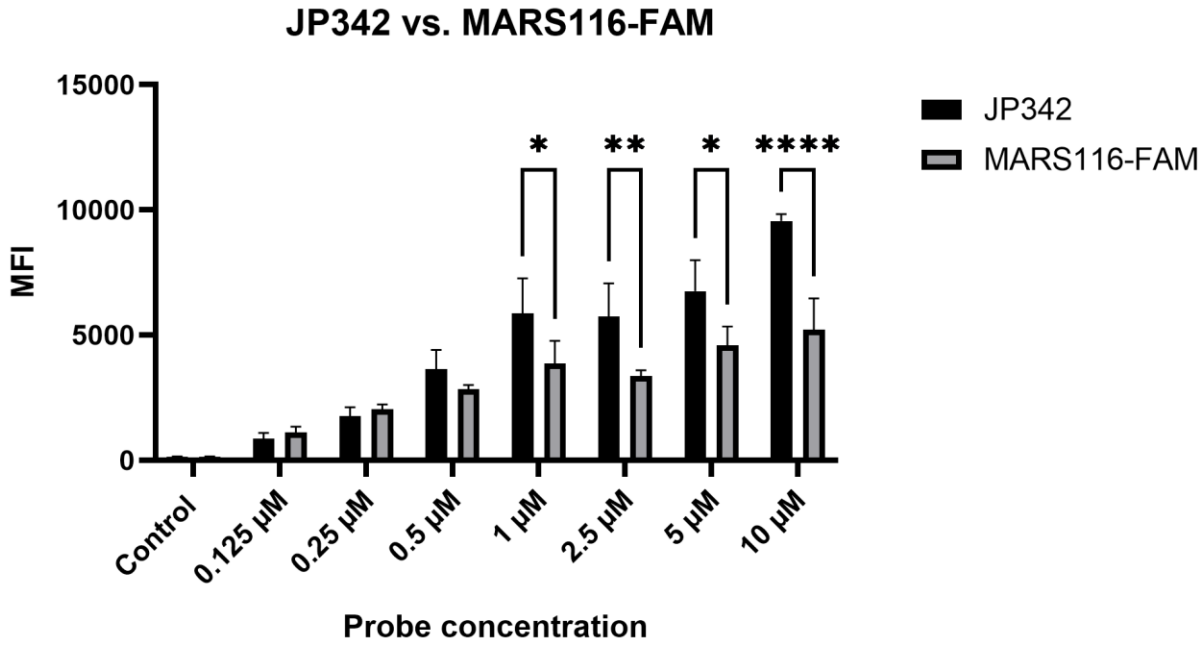

Figure 8. Comparison of JP342 and MARS116-FAM probes for CatG detection using flow cytometry analysis. Median fluorescence intensity (MFI) values were obtained using JP342 and MARS116-FAM probes across 7 concentrations. Data was analyzed using 2-way ANOVA and Sidak post hoc test with significance shown at each probe concentration (* $p \leq 0.05$, **$p \leq 0.01$, **** $p \leq 0.0001$).Values represent mean ± SD, n = 3.

In the presence of CatG inh I (Figure 9), fluorescence intensity was markedly reduced for both probes across all used concentrations. Furthermore, it was observed that JP342 demonstrated a higher fluorescent signal at multiple concentrations in comparison to MARS116-FAM, especially at 10 µM, where the difference between the two probes remained significant. The reduction of MFI by using the CatG inh I shows the specificity of the probes for CatG activity.

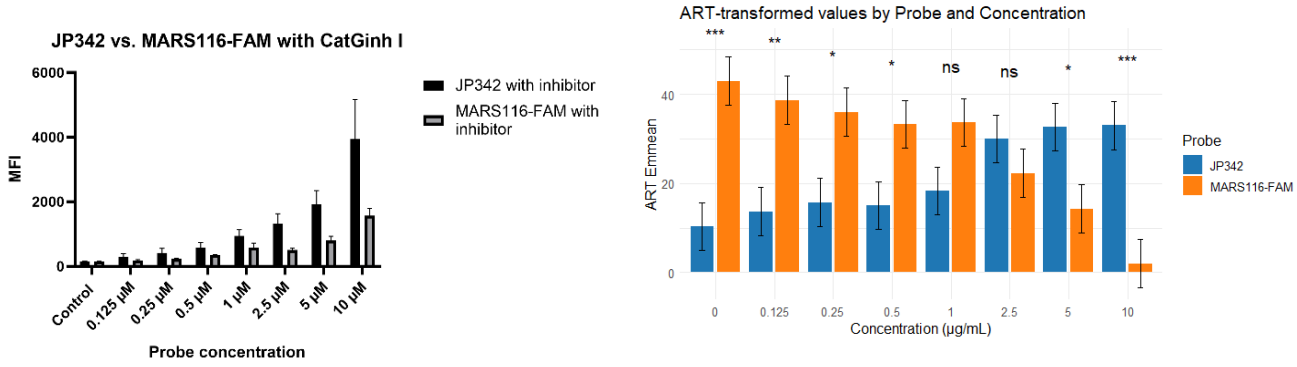

Figure 9. Flow cytometry-based comparison of JP342 and MARS116-FAM probes in the presence of CatG inh I across 7 concentrations. The left panel shows raw MFI values, and the right panel displays ART-transformed estimated marginal means (emmeans ± SE) to account for data distribution. Statistical analysis was performed using aligned rank transform (ART) to account for data distribution. Significant differences between probes at each concentration are indicated: (* $p \leq 0.05$, ** $p \leq 0.01$, *** $p \leq 0.001$), $n = 3$.

4.4 MARS116-FAM labels CatG with higher affinity in contrast to JP342 in A549 cells analyzed via confocal microscopy

Based on the confocal images, it can be observed that both the novel probe JP342 and the established MARS116-FAM successfully detected CatG activity in A549 cells, as indicated by green fluorescence. In untreated control cells incubated with 5 µM probe (no CatG), no green fluorescence was observed for either probe. However, with the treatment of A549 with CatG, it can be seen that both probes displayed increased green fluorescence signals in a concentration-dependent manner. At 5 µM, signal intensity was greater than at 2.5 µM for both probes. In the presence of the CatG inh I [50 µM], green fluorescence was significantly reduced for JP342-incubated cells, whereas A549 cells treated with MARS116-FAM retained some

residual signal (Figure 10). Additionally, supplementary confocal images (Supplementary Figure 1) confirm that JP342, like MARS116-FAM, detects CatG both on the membrane and intracellularly. In conclusion, MARS116-FAM binds with higher affinity to the catalytic center of CatG in contrast to JP342 analyzed by confocal microscopy.

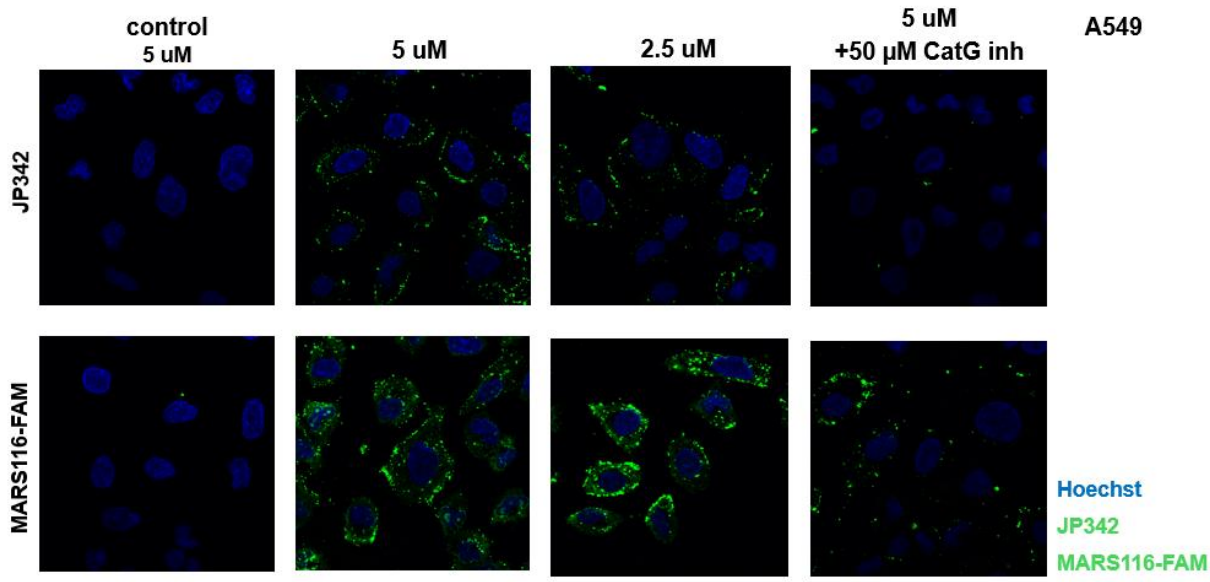

Figure 10. Confocal microscopy images showing CatG detection in A549 cells using JP342 and MARS116-FAM probes. The image displays the localization of exogenously added CatG [10 µg/mL] under serum-free conditions. Hoechst dye was used to stain nuclei (blue), and green fluorescence indicates probe functionality, n = 2.

5 DISCUSSION

This study aimed to evaluate and compare the performance of two activity-based probes, JP342 and MARS116-FAM, for detecting CatG activity in A549 cells using gel electrophoresis (SDS-PAGE), flow cytometry, and confocal microscopy. Furthermore, the application of the apoptosis profile array (Figure 4) ensured that exogenous purified CatG could be introduced into A549, as no apoptotic markers such as caspase-3 or survivin were upregulated in the treated samples. Hence, the probes' functionality could be properly assessed for other experimental applications.

As for SDS-PAGE analysis, the results demonstrated that MARS116-FAM showed stronger fluorescent signals than JP342 across both protease titration (Figure 5) and probe titration (Figure 6) experiments. This indicates the greater sensitivity of MARS116-FAM for detecting proteolytically active CatG in this experimental setting. Thus, MARS116-FAM has a higher affinity to the catalytic center of CatG in contrast to JP342. Similar results were observed for MARS116-FAM in the study of Schroeder et al. (2019), which demonstrated that MARS116-FAM delivers strong and reliable CatG labeling in SDS-PAGE, hence confirming its effectiveness in biochemical applications.

For inhibitor validation (Figure 7), it further confirmed that both probes are specific for active CatG. However, a faint residual band was still visible with MARS116-FAM at 10 μM in the presence of the CatG inh I, which could be possible due to an excess probe or, most likely, the higher affinity of MARS116-FAM over the CatG inh I. Despite this, the overall reduction in signal supports the specific activity-dependent nature of both activity-based probes.

The results from confocal imaging (Figure 10) support the data from SDS-PAGE that MARS116-FAM is a more potent and highly sensitive activity-based probe. Moreover, the persistence of fluorescence from MARS116-FAM in the presence of CatG inh I suggests that this probe may exhibit some off-target activity. This could be due to factors such as fluorophore instability or the higher affinity of MARS116-FAM over the CatG inh I. In contrast, JP342 displayed a minimal signal under inhibition, which indicates its specificity and dependence on active CatG. Furthermore, data from Figure 10 suggested that JP342 primarily labeled membrane-associated CatG, however, supplementary images (Supplementary Figure 1) revealed that it also detects intracellular protease, similar to MARS116-FAM (Assylbekova et al., 2024). Overall, these findings highlight potential limitations in the use of MARS116-FAM for inhibitor-based assays.

In contrast, flow cytometry results revealed that JP342 consistently generated higher median fluorescence intensity (MFI) than MARS116-FAM, particularly at concentrations ≥1 µM. This trend was observed for both with (Figure 9) and without inhibitor (Figure 8) treatments, which suggests a more efficient or stable binding to active CatG by JP342 on the cell surface, resulting in higher probe retention. JP342 incorporates a BODIPY-FL fluorophore, which could potentially affect the binding capacity of the probe to the catalytic center of CatG in a cellular environment due to its unique hydrophobic properties, making it ideal for staining lipids and membranes (Thermo Fisher Scientific, 2024). Although JP342 has not yet been described in published literature, it was kindly provided by Professor Verhelst and used in its fully labeled, fluorescent form. Its design likely builds on ongoing work in his lab developing activity-based probes using bioorthogonal chemistry, as shown in earlier studies on protease detection (Verhelst et al., 2020). It can be suggested that this hydrophobicity can lead to lower background fluorescence and higher signal-to-noise ratios in certain applications, such as flow cytometry. Structurally, the stable nature of BODIPY-FL, along with potential differences in linker conformation and structure (e.g, triazole ring), may enhance JP342's ability to remain bound to cell-surface CatG more efficiently under PBS conditions. These characteristics could likely explain the higher MFI values observed for JP342 on A549 cells. The diminished signal following inhibitor treatment with flow cytometry supports other data that both probes bind specifically to active CatG. The residual fluorescence signal observed with JP342, even in the presence of the CatG inh I, could also indicate a higher binding affinity for this experimental setup with flow cytometry rather than nonspecificity. This is also supported by the SDS-PAGE, where inhibitor-based controls in the gel did not reveal significant labeling.

Taken together, the data highlight that while MARS116-FAM offers superior signal intensity in gel-based and imaging applications, JP342 might be better suited in flow cytometry, likely due to differences in probe accessibility, retention, or fluorophore properties. These findings underscore the critical significance of selecting probes for the detection of protease activity in the respective assay.

Limitations and Future Directions

The directly fluorescent ABPs, such as MARS116-FAM and JP342 are versatile tools and beneficial for *in vitro* experiments, as the excess of the unbound probe can be washed away (e.g. in preparation of samples for flow cytometry). They have a simple design (Figure 3), can utilize different dyes, are straightforward to use, and can immediately detect labeled enzymes. The fluorescent tag bound to the protease can be visualized through gels or microscopy without

needing an additional activation step (Burster et al., 2021). However, for *in vivo* applications, such probes can produce high background signals because they are fluorescent even in their unbound state, which makes it difficult to distinguish specific labeling of active protease from non-specific probe accumulation. In contrast, quenched ABPs are designed to emit fluorescence only upon covalent binding to their target enzyme, thus offering far greater spatial specificity by minimizing the background interference from the unbound probe (Serim et al., 2014). In future work, incorporating a quenched CatG probe could offer deeper insights into protease localization and enable more accurate live-cell imaging. This would be particularly valuable for investigating CatG activity in tumor microenvironments or inflammation, where CatG is involved.

6 BIBLIOGRAPHY

Assylbekova, A., Allayarova, M., Konysbekova, M., Bekturgan, A., Makhanova, A., Brown, S., Grzegorzek, N., Kalbacher, H., Kalendar, R., & Burster, T. (2024). The proteolytic activity of Neutrophil-Derived serine proteases bound to the cell surface arming lung epithelial cells for viral defense. *Molecules*, *29*(18), 4449. https://doi.org/10.3390/molecules29184449

Bittel, A. M., Davis, A. M., Wang, L., Nederlof, M. A., Escobedo, J. O., Strongin, R. M., & Gibbs, S. L. (2018). Varied Length Stokes Shift BODIPY-Based fluorophores for multicolor microscopy. *Scientific Reports*, *8*(1). https://doi.org/10.1038/s41598-018-22892-8

Burster, T., Gärtner, F., Knippschild, U., & Zhanapiya, A. (2021). Activity-Based probes to utilize the proteolytic activity of cathepsin G in biological samples. *Frontiers in Chemistry*, *9*. https://doi.org/10.3389/fchem.2021.628295

Brehm, A., Geraghty, P., Campos, M., Garcia-Arcos, I., Dabo, A. J., Gaffney, A., Eden, E., Jiang, X. C., D'Armiento, J., & Foronjy, R. (2014). Cathepsin G degradation of phospholipid transfer protein (PLTP) augments pulmonary inflammation. *FASEB journal : official publication of the Federation of American Societies for Experimental Biology*, *28*(5), 2318–2331. https://doi.org/10.1096/fj.13-246843

Conus, S., & Simon, H. (2010). Cathepsins and their involvement in immune responses. *Schweizerische Medizinische Wochenschrift*. https://doi.org/10.4414/smw.2010.13042

Fang, H., Peng, B., Ong, S. Y., Wu, Q., Li, L., & Yao, S. Q. (2021). Recent advances in activity-based probes (ABPs) and affinity-based probes (AfBPs) for profiling of enzymes. *Chemical Science*, *12*(24), 8288–8310. https://doi.org/10.1039/d1sc01359a

Korkmaz, B., Horwitz, M. S., Jenne, D. E., & Gauthier, F. (2010). Neutrophil elastase, proteinase 3, and cathepsin G as therapeutic targets in human diseases. *Pharmacological reviews*, *62*(4), 726–759. https://doi.org/10.1124/pr.110.002733

Kurup, R., & Patel, S. (2017). Neutrophils in acute coronary syndrome. *EMJ Cardiology*, 79–87. https://doi.org/10.33590/emjcardiol/10314937

Matin, M. M., Matin, P., Rahman, M. R., Hadda, T. B., Almalki, F. A., Mahmud, S., Ghoneim, M. M., Alruwaily, M., & Alshehri, S. (2022). Triazoles and their derivatives: chemistry, synthesis, and therapeutic applications. *Frontiers in Molecular Biosciences*, *9*. https://doi.org/10.3389/fmolb.2022.864286

Miyata, J., Tani, K., Sato, K., Otsuka, S., Urata, T., Lkhagvaa, B., Furukawa, C., Sano, N., & Sone, S. (2006). Cathepsin G: the significance in rheumatoid arthritis as a monocyte

chemoattractant. *Rheumatology International*, *27*(4), 375–382. https://doi.org/10.1007/s00296-006-0210-8

Ortega-Gomez, A., Salvermoser, M., Rossaint, J., Pick, R., Brauner, J., Lemnitzer, P., Tilgner, J., De Jong, R. J., Megens, R. T. A., Jamasbi, J., Döring, Y., Pham, C. T., Scheiermann, C., Siess, W., Drechsler, M., Weber, C., Grommes, J., Zarbock, A., Walzog, B., & Soehnlein, O. (2016b). Cathepsin G controls arterial but not venular myeloid cell recruitment. *Circulation*, *134*(16), 1176–1188. https://doi.org/10.1161/circulationaha.116.024790

Pham, C. T. N. (2006). Neutrophil serine proteases: specific regulators of inflammation. *Nature Reviews. Immunology*, *6*(7), 541–550. https://doi.org/10.1038/nri1841

Rayes, T. E., Catena, R., Lee, S., Stawowczyk, M., Joshi, N., Fischbach, C., Powell, C. A., Dannenberg, A. J., Altorki, N. K., Gao, D., & Mittal, V. (2015). Lung inflammation promotes metastasis through neutrophil protease-mediated degradation of Tsp-1. Proceedings of the National Academy of Sciences, 112(52), 16000–16005. https://doi.org/10.1073/pnas.1507294112

Schroeder, R., Grzywa, R., Wirtz, C. R., Sienczyk, M., & Burster, T. (2019). Application of a novel FAM-conjugated activity-based probe to determine cathepsin G activity intracellularly. *Analytical Biochemistry*, *588*, 113488. https://doi.org/10.1016/j.ab.2019.113488

SDS Page Protocol - NeoBiotechnologies. (2024, May 23). NeoBiotechnologies. https://www.neobiotechnologies.com/protocol/sds-page-protocol/?srsltid=AfmBOooK7zKEudPHg84HyLEe_k3KkvMIRd2TneB9XwOH7AaR50tXwJcv

Serim, S., Baer, P., & Verhelst, S. H. L. (2014). Mixed alkyl aryl phosphonate esters as quenched fluorescent activity-based probes for serine proteases. *Organic & Biomolecular Chemistry*, *13*(8), 2293–2299. https://doi.org/10.1039/c4ob02444c

Sionov, R. V., Fainsod-Levi, T., Zelter, T., Polyansky, L., Pham, C. T., & Granot, Z. (2019). Neutrophil cathepsin G and tumor cell RAGE facilitate Neutrophil Anti-Tumor cytotoxicity. *OncoImmunology*, *8*(9), e1624129. https://doi.org/10.1080/2162402x.2019.1624129

Swain, C. (2012). *Serine protease inhibitors | Cambridge MedChem Consulting*. https://www.cambridgemedchemconsulting.com/resources/hit_identification/focus/serine_protease_inhibitors.html

Thermo Fisher Scientific. (2024). *BODIPY FL*. https://www.thermofisher.com/kz/en/home/life-science/cell-analysis/fluorophores/bodipy-fl.html?SID=fr-bodipy-main

Verhelst, S. H. L., Bonger, K. M., & Willems, L. I. (2020). Bioorthogonal reactions in Activity-Based protein profiling. *Molecules*, *25*(24), 5994. https://doi.org/10.3390/molecules25245994

Zamolodchikova, T. S., Tolpygo, S. M., & Svirshchevskaya, E. V. (2020). Cathepsin G—Not only inflammation: the immune protease can regulate normal physiological processes. *Frontiers in Immunology*, *11*. https://doi.org/10.3389/fimmu.2020.00411

Supplementary materials

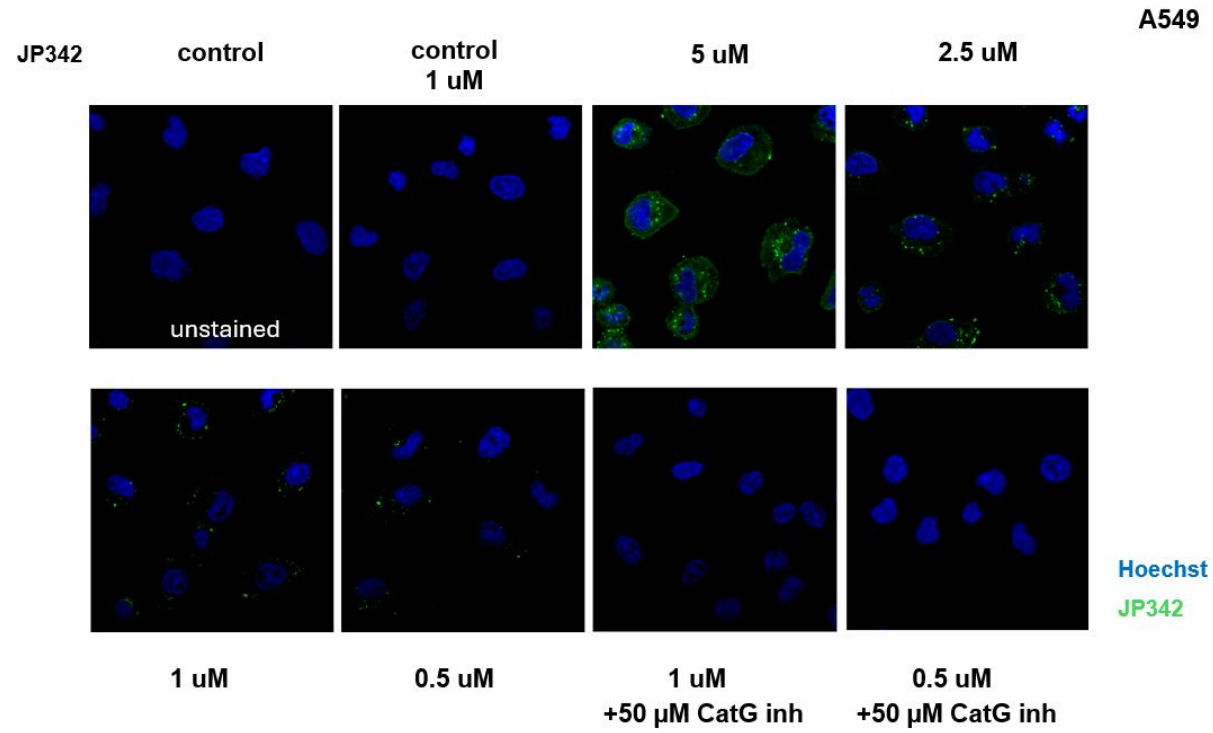

Supplementary Figure 1. Representative confocal images showing A549 cells incubated with JP342 at various concentrations [0.5–5 µM] in serum-free conditions. Nuclei were counterstained with Hoechst dye (blue), and the JP342 signal is shown in green. Control samples include unstained cells (no CatG and probe) and cells incubated with a probe in the absence of CatG, n = 1.